*Acta Cryst.* (1996). B52, 662–667

# Experimental and Theoretical Morphologies of Diuron, *N'*-(3,4-Dichlorophenyl)-*N,N*-Dimethylurea

GUILLAUME PFEFER AND ROLAND BOISTELLE*

*Centre de Recherche sur les Mécanismes de la Croissance Cristalline-CNRS,† Campus Luminy, Case 913, F-13288 Marseille CEDEX 9, France*

(*Received 20 July 1995; accepted 15 January 1996*)

## Abstract

Crystals of diuron, *N'*-(3,4-dichlorophenyl)-*N,N*-dimethylurea, $C_9H_{10}Cl_2N_2O$, were grown from ethanol at low supersaturation. The crystal faces were indexed using a two-circle optical goniometer and X-ray diffraction was used to orientate the crystal morphology with respect to the unit cell. The experimental morphologies were compared with the morphologies predicted by the BFDH (Bravais, Friedel, Donnay, Harker) and attachment energy (AE) methods and calculated from two crystal structures. Good agreement was obtained between experimental and theoretical habits, despite the fact that the crystals exhibit 27 faces belonging to 13 crystallographic forms.

## 1. Introduction

Diuron, *N'*-(3,4-dichlorophenyl)-*N,N*-dimethylurea, is an agrochemical molecule generally used as a weed killer. Single and well faceted crystals of diuron were grown from ethanol at low supersaturation. They exhibited a thick rod-like habit with numerous terminal faces. Diuron is monoclinic, space group $P2_1/a$, with $a = 9.191$, $b = 14.632$, $c = 7.738$ Å, $\beta = 101.32°$ (Cadiergue, 1992), but other data exist in the literature (Baughman, Sams, Helland & Jacobson, 1980). From optical measurements and X-ray diffraction patterns it was possible to determine the experimental morphology of the crystals in order to compare it to the theoretical morphology. Previous studies, devoted to morphology predictions, demonstrated the efficiency of two methods. The first is based on geometrical considerations (Bravais, Friedel, Donnay, Harker), *i.e.* the BFDH method (Bravais, 1913; Friedel, 1907; Donnay & Harker, 1937), while the second gives a better prediction from interaction energies between growth units and crystal faces, *i.e.* periodic bond chain and attachment energy methods (Hartman & Perdok, 1955*a,b*; Hartman & Bennema, 1980; Berkovitch-Yellin, 1985). Several papers illustrated the efficiency of these approaches in the case of inorganic (Hartman, 1980; Woensdregt, 1992) and organic crystals (Black, Davey & McLean, 1988; Black *et al.*, 1990; Docherty, Clydesdale, Roberts & Bennema, 1991), although some others demonstrated that theoretical morphologies should take into account solvent effects (Davey *et al.*, 1992; Van der Voort, 1990).

In the present study we calculated the morphologies of diuron using BFDH and attachment energy models. We aimed first at comparing experimental and predicted morphologies and second at showing how small discrepancies in the calculations induce important modifications in the predicted morphologies.

## 2. Experimental morphology of diuron

The solubility '*s*' of diuron in pure ethanol was determined at 293 K; $s(293\text{ K}) = 2.7$ g per 100 g ethanol. Crystallization was achieved at 293 K in slightly supersaturated solutions. Supersaturation ranged from 5 to 20% in order to grow crystals within 1 or 2 d. The crystals always exhibited a thick rod-like habit with numerous terminal faces; a typical crystal of diuron is shown in Fig. 1. The number and nature of the terminal faces are very dependent on the growth conditions (proximity of other crystals, presence of traces of impurities *etc.*). X-ray diffraction measurements, using a precession camera, were made to determine the elongation axis and rapidly find out the indices of the largest lateral faces. It turned out that the elongation axis is the reciprocal $a^*$ axis and that the large basal plane is 001. The number of terminal faces is very important, since *ca* ten faces having almost the same morphological importance appear on both crystal extremities. The angles between the normals to the different faces were calculated from optical determinations using a two-circle goniometer. They are given in Table 1. The crystal symmetry is consistent with the point group $P2_1/a$, although we note some dissymmetries in the morphological importance of 110 and $\bar{1}\bar{1}0$ and the existence of 131 only on the left side of the crystal. The difference between the two extremities can be explained by small differences in the environment of the crystal during growth. Full indexing is given in Table 2 and Fig. 2 was drawn by means of the program *SHAPE* (Dowty, 1980).

† Associated with the Universities Aix-Marseille II and III.

## 3. Theoretical morphology

Both BFDH (Bravais, 1913; Friedel, 1907; Donnay & Harker, 1937) and AE (Hartman & Perdock 1955*a*,*b*; Hartman & Bennema, 1980; Berkovitch-Yellin, 1985) methods were used to calculate the theoretical morphology.

### 3.1. *The BFDH method*

This method is grounded on the assumption that the relative development of a face is proportional to its interplanar $d$ spacing, taking into account the absence of the diffraction peaks imposed by the space group. In the space group $P2_1/a$ the spacings of 010 and 100 must be divided by two as only 020 and 200 peaks exist on the diffraction patterns. This semi-empirical method is very simple because it requires only the knowledge of the cell parameters and space group. However, the BFDH approach does not take into consideration the chemical and physical nature of the material. Here we calculated the interplanar spacings and used the so-called Wulff plot (Wulff, 1901) to draw the crystal habit. In this representation the crystal shape is the smallest polyhedron obtained from the $d$ spacings. The $d$ spacings are given in Table 3 and the corresponding morphology in Fig. 3.

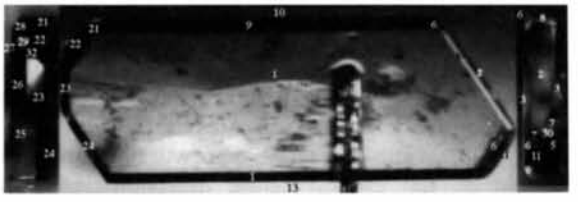

Fig. 1. Optical micrograph of diuron showing the experimental morphology after crystallization from ethanol at low supersaturation.

Table 1. *Angles between the normals to the crystal faces determined experimentally and calculated from the cell parameters*

| Face numbers in Fig. 1 | Angles (exp.) (°) | Angles (calc.) (°) |
|---|---|---|
| | Left side in Fig. 1 (B–B in Fig. 2) | |
| 1/12 | 27.20 | 27.24 |
| 1/9 | 27.00 | 27.24 |
| 10/1 | 89.93 | 90.00 |
| 9/2 | 67.40 | 67.03 |
| 12/24 | 40.04 | 40.14 |
| 2/24 | 129.84 | 129.48 |
| 25/1 | 99.33 | 99.37 |
| 23/1 | 67.77 | 67.55 |
| 26/23 | 33.39 | 33.23 |
| 32/1 | 68.58 | 68.51 |
| 32/25 | 57.34 | 57.35 |
| 28/1 | 97.05 | 97.06 |
| 28/5 | 128.86 | 129.06 |
| 28/8 | 78.02 | 78.08 |
| 21/26 | 70.50 | 70.39 |
| 21/22 | 28.85 | 29.07 |
| 21/23 | 56.04 | 56.23 |
| | Right side in Fig. 1 (A–A in Fig. 2) | |
| 1/2 | 80.63 | 80.22 |
| 1/3′ | 39.91 | 39.55 |
| 1/3 | 130.68 | 130.34 |
| 1/8 | 82.70 | 82.53 |
| 2/11 | 63.38 | 63.15 |
| 1/5 | 130.77 | 130.34 |
| 8/5 | 89.56 | 89.48 |
| 1/7″ | 121.83 | 111.09 |
| 2/7″ | 34.10 | 33.60 |
| 7/2 | 32.97 | 31.38 |
| 7/5 | 59.43 | 59.47 |
| 7/8 | 51.00 | 50.55 |
| 30/2 | 44.65 | 44.41 |
| 30/5 | 32.86 | 32.48 |
| 6′/2 | 78.64 | 78.53 |
| 6″/2 | 36.27 | 35.59 |
| 6″/1 | 48.48 | 48.41 |

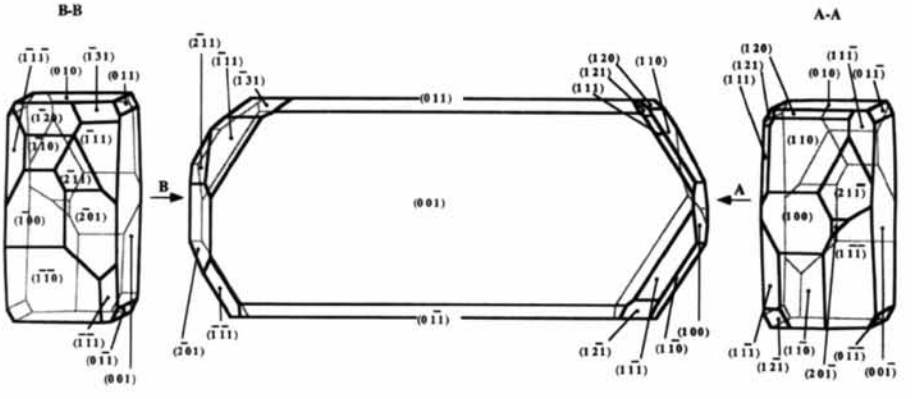


Fig. 2. Face indices deduced from optical analysis and angle calculation.

Table 2. *Relationship between face numbers and indices given in Figs. 1 and 2, respectively*

| | | |
|---|---|---|
| 1 = (00$\bar{1}$) | 11 = (1$\bar{1}$0) | 23 = ($\bar{2}$0$\bar{1}$) |
| 1′ = (00$\bar{1}$) | 25 = ($\bar{1}$10) | 7″ = (21$\bar{1}$) |
| 7 = ($\bar{1}$00) | 3′ = ($\bar{1}$11) | 32 = ($\bar{2}$11) |
| 26 = ($\bar{1}$00) | 27 = ($\bar{1}$1$\bar{1}$) | 6′ = (1$\bar{2}$1) |
| 10 = (0$\bar{1}$0) | 3 = (11$\bar{1}$) | 6″ = (121) |
| 13 = (0$\bar{1}$0) | 5 = (1$\bar{1}$$\bar{1}$) | 8 = ($\bar{1}$20) |
| 9 = (011) | 24 = ($\bar{1}$11) | 28 = ($\bar{1}$20) |
| 12 = (0$\bar{1}$1) | 22 = ($\bar{1}$11) | 2 = ($\bar{1}$10) |
| 14 = (0$\bar{1}$1) | 30 = (20$\bar{1}$) | 21 = ($\bar{1}$31) |

Table 3. *Interreticular spacings and attachment energies from which are deduced the relative growth rates of the faces: normalization with respect to the largest d or the smallest $E_{att}$*

| Forms | $d_{hkl}$ (Å) | $E_{att}$ (kJ mol$^{-1}$) | Relative growth rates BFDH | $E_{att}$ |
|---|---|---|---|---|
| {020} | 7.316 | 49.78 | 1.049 | 1.00 |
| {011} | 6.736 | 61.36 | 1.139 | 1.23 |
| {021} | 5.266 | 76.54 | 1.457 | 1.54 |
| {001} | 7.587 | 54.26 | 1.011 | 1.09 |
| {200} | 4.506 | 105.67 | 1.703 | 2.12 |
| {20$\bar{1}$} | 4.259 | 126.57 | 1.802 | 2.54 |
| {120} | 5.680 | 82.26 | 1.351 | 1.65 |
| {110} | 7.673 | 73.90 | 1.000 | 1.48 |
| {11$\bar{1}$} | 4.994 | 99.82 | 1.536 | 2.00 |
| {111} | 5.912 | 96.06 | 1.298 | 1.93 |
| {12$\bar{1}$} | 4.844 | 104.50 | 1.584 | 2.10 |
| {121} | 4.299 | 101.03 | 1.785 | 2.03 |
| {21$\bar{1}$} | 4.089 | 129.50 | 1.876 | 2.60 |
| {$\bar{1}$31} | 3.893 | 113.24 | 1.971 | 2.27 |

### 3.2. *The AE method*

This approach, based on molecular mechanics, involves the calculation of the interaction energies between, on the one hand, a growth unit adsorbed in a crystallographic position on an *hkl* face and, on the other hand, (i) its neighbours in the same slice of thickness $d_{hkl}$, taking into account the extinction conditions of the space group; (ii) all molecules of a semi-infinite crystal limited by the actual *hkl* face. The corresponding energies are termed $E_{sl}$ and $E_{att}$, respectively. In addition, from the interaction energy between a molecule located at the centre of the crystal and all its neighbours, it is possible to deduce the crystal energy ($E_{cr}$). The attachment energy formalism is grounded on the assumption that the growth rate of a face is proportional to $E_{att}$: the greater $E_{att}$, the faster the growth rate and the smaller the extension of the face on the crystal morphology. Since the calculations are made as if the crystal were in the vapour phase, they do not provide good results in the case of specific solvation of some crystal faces (Davey *et al.*, 1992). Slice and attachment energies are related to the lattice energy by

$$E_{cr} = E_{sl} + 2E_{att}. \quad (1)$$

In our study we used the structural data (Cadiergue, 1992; Baughman, Sams, Helland & Jacobson, 1980) and the program *BIOSYM* (Biosym Technologies, 1993) to build (i) a large crystal to calculate $E_{cr}$ and (ii) crystal slices of thickness $d_{hkl}$ to calculate $E_{sl}$; $E_{att}$ is deduced from both quantities by means of (1). The atomic coordinates (Cadiergue, 1992) are given in Table 4. The program calculates the atom–atom interactions using Lennard-Jones 6–12 (Lennard-Jones, 1924) and Coulombic potentials. The Lennard-Jones parameters are directly taken from the *BIOSYM* forcefield CVFF (Dauber-Osguthorpe *et al.*, 1988). Partial atomic charges are calculated using the *ab initio* quantum chemistry program *GAUSSIAN*92 with the CHELPG method (Wiberg & Breneman, 1990) on the 6-31 G** basis. The largest interatomic distance for the calculations was 30 Å. The resulting crystal morphology was built using Wulff's method (Wulff, 1901) and drawn by means of the program *SHAPE* (Dowty, 1980). Attachment energies and relative growth rates are given in Table 3, the corresponding morphologies being displayed in Fig. 4(*a*) (data of Cadiergue, 1992) and (*b*) (data of Baughman, Sams, Helland & Jacobson, 1980). We see that one more form, {$\bar{1}$11}, occurs on Fig. 4(*b*).

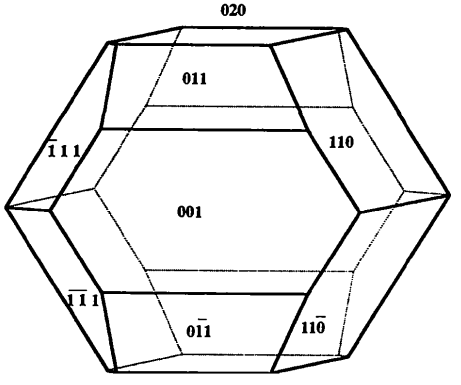


Fig. 3. Morphology deduced from the BFDH model.

## 4. Discussion

The comparison between the BFDH and $E_{att}$ morphologies of diuron (Figs. 3 and 4) illustrates the fundamental difference between the two approaches. The BFDH model gives rise to a morphology determined on pure geometrical criteria. The $E_{att}$ model combines structural and energetical data. The BFDH habit is less elongated than the $E_{att}$ habit. This difference is easily explained by examination of the structure by means of a projection along the *c* axis, which shows one periodic bond chain (hydrogen bonds) parallel to [100], which is precisely the zone axis of the diuron crystals shown in Figs. 1 and 2. BFDH calculations do not consider this pecularity. However, the most striking fact is that

Table 4. *Atomic coordinates of diuron taken from the thesis by Cadiergue (1992)*

| | *x* | *y* | *z* |
|---|---|---|---|
| Cl1 | 0.4034 | 0.4578 | −0.8256 |
| Cl2 | 0.2214 | 0.5392 | −0.5534 |
| C3 | 0.3869 | 0.3989 | −0.6346 |
| C4 | 0.3030 | 0.4337 | −0.5187 |
| C5 | 0.2878 | 0.3839 | −0.3735 |
| C6 | 0.3531 | 0.2998 | −0.3396 |
| C7 | 0.4389 | 0.2655 | −0.4573 |
| C8 | 0.4508 | 0.3169 | −0.6041 |
| N9 | 0.3296 | 0.2514 | −0.1922 |
| C10 | 0.4247 | 0.1901 | −0.0996 |
| O11 | 0.5467 | 0.1734 | −0.1351 |
| N12 | 0.3788 | 0.1507 | 0.0378 |
| C13 | 0.4767 | 0.0899 | 0.1514 |
| C14 | 0.2302 | 0.1616 | 0.0756 |
| H15 | 0.2222 | 0.4116 | −0.2824 |
| H16 | 0.4948 | 0.1999 | −0.4335 |
| H17 | 0.5142 | 0.2897 | −0.6979 |
| H18 | 0.2316 | 0.2632 | −0.1499 |
| H19 | 0.4490 | 0.0900 | 0.2820 |
| H20 | 0.4647 | 0.0211 | 0.0973 |
| H21 | 0.5909 | 0.1125 | 0.1609 |
| H22 | 0.2052 | 0.2339 | 0.0835 |
| H23 | 0.1496 | 0.1302 | −0.0291 |
| H24 | 0.2247 | 0.1289 | 0.2006 |

neither morphology of Figs. 3 and 4 exhibit the numerous terminal faces which occur on the experimental morphology. However, the theoretical habits exhibit predominant 001, 010 and 011 forms on the zone axis [100] and the most extended terminal form 110, in agreement with the experimental morphology. We note (Table 3) that the attachment energies of some terminal faces are not significantly different from each other, so that small modifications in these energies may induce the appearance of some new faces and the disappearance of some others. Moreover, during crystallization, small fluctuations in supersaturation and temperature or small amounts of impurities are able to produce significant modifications in the relative development of the facets. To illustrate the influence of such effects, we have increased the attachment energy of the faces of the 110 form by 10% and decreased the attachment energy of the other terminal faces also by 10%. The modified morphologies are shown in Figs. 5(*a*) and (*b*). There are two more terminal forms, 120 and $\bar{1}11$, in Fig. 5(*a*) (structural data of Cadiergue, 1992) and also two more forms on Fig. 5(*b*), 120 and 111. Both forms are observed on the experimental morphology. 100, 121 and $12\bar{1}$ are just at the border of these morphologies. It is quite clear that 10% is a large variation of $E_{att}$, but it is noteworthy that the calculations are extremely dependent on the accuracy of the crystal structure, *i.e.* on the atomic coordinates. As an example, the value of $E_{cr}$ is ~9% larger, if calculated from the data by Baughman, Sams, Helland & Jacobson (1980), than the value calculated from the data of Cadiergue (1992).

For concluding remarks we can also consider the possible errors arising from the model. Independently from the attachment energy theory, the predicted morphology can be affected by the potentials and

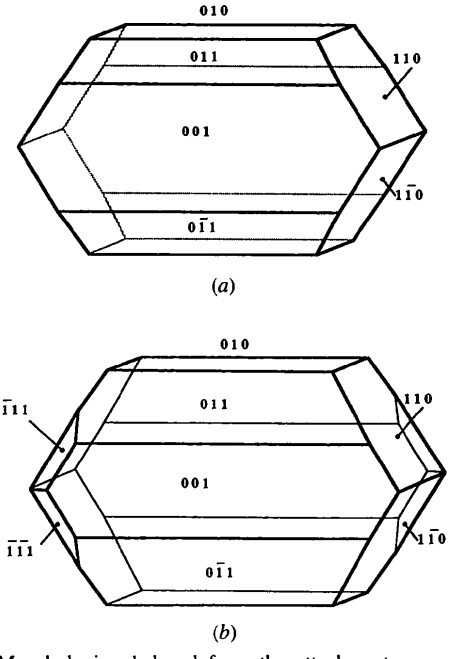


Fig. 4. Morphologies deduced from the attachment energy model, with structural data of (*a*) Cadiergue (1992) and (*b*) Baughman, Sams, Helland & Jacobson (1980)

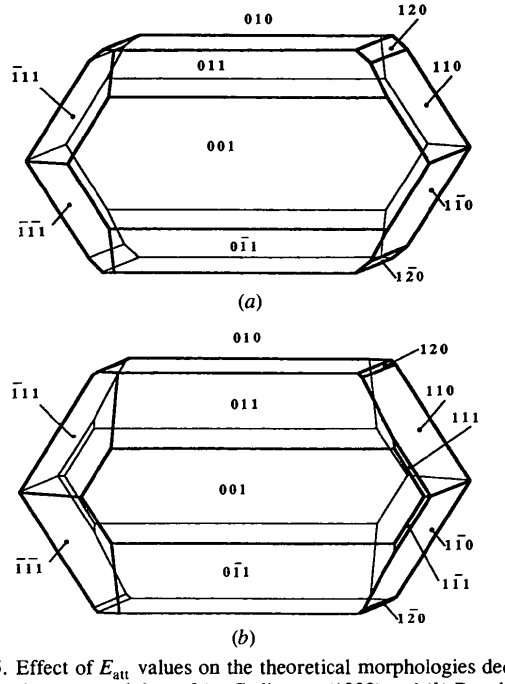


Fig. 5. Effect of $E_{att}$ values on the theoretical morphologies deduced from the structural data of (*a*) Cadiergue (1992) and (*b*) Baughman, Sams, Helland & Jacobson (1980).

charges used to calculate $E_{cr}$, $E_{sl}$ and $E_{att}$. One possibility to check the validity of the calculations is to compare $E_{cr}$ with the enthalpy of sublimation obtained from direct calorimetry measurements (Bondi, 1968). The crystal energy can be related to the sublimation enthalpy by

$$1/2|E_{cr}| = \Delta_{sub}H(0\ \mathrm{K}) = \Delta_{sub}H(T\ \mathrm{K}) + \int_0^T [C_p^{sol} - C_p^{vap}]\mathrm{d}T. \quad (2)$$

This equation is often approximated (Bondi, 1968) by

$$1/2|E_{cr}| = \Delta_{sub}H(0\ \mathrm{K}) \approx \Delta_{sub}H(T\ \mathrm{K}) + 2RT. \quad (3)$$

The sublimation enthalpy, determined experimentally (Pfefer, Boistelle & Sabbah, 1996), is $133.88 \pm 0.17\,\mathrm{kJ\,mol^{-1}}$ at 298 K. After temperature correction we obtain $\Delta_{sub}H(0\ \mathrm{K}) = 138.82\,\mathrm{kJ\,mol^{-1}}$. This value is to be compared with $1/2|E_{cr}| = 152.6\,\mathrm{kJ\,mol^{-1}}$, a value obtained with a spherical crystal of radius 30 Å using the data of Cadiergue (1992). Increasing the radius of the crystal did not significantly affect the lattice energy, which checks the convergence of the calculations as shown in Fig. 6. Because of the use of neutral molecules, we avoid the summation difficulties encountered in particular in the case of inorganic crystals. The disagreement of 10% between measured and calculated heat of sublimation could be explained by the use of the general forcefield CVFF in the particular case of diuron and also by the temperature correction. It could also explain, at least partially, the disagreement between experimental and theoretical morphologies. However, the solvent probably also affects the morphology. This effect is not taken into account by the calculation.

## 5. Conclusions

In the present study we determined the experimental morphology of diuron and used the BFDH and $E_{att}$ models to obtain its theoretical morphology. The overall agreement between calculated and experimental habits is quite good, taking into account that the crystal exhibited 27 faces belonging to 13 crystallographic forms. However, there are some discrepancies concerning small terminal facets. Even if there are some uncertainties on the $E_{att}$ energies, the validity of the calculations, in particular of the forcefield CVFF, was demonstrated by comparing $E_{cr}$ and $\Delta_{sub}H$. However, the models do not consider the effects of external parameters such as solvent, impurities, supersaturation and temperature, which are able to modify the crystal morphology. This is especially valid for the terminal faces, the extension of which can be modified by small differences in their growth rates. The calculation of the attachment energies confirms this point as the terminal faces exhibit attachment energies very close to each other. A study is in progress where we try to adjust a forcefield on the particular case of diuron. In the future we also project to take solvent adsorption into account for morphology prediction.

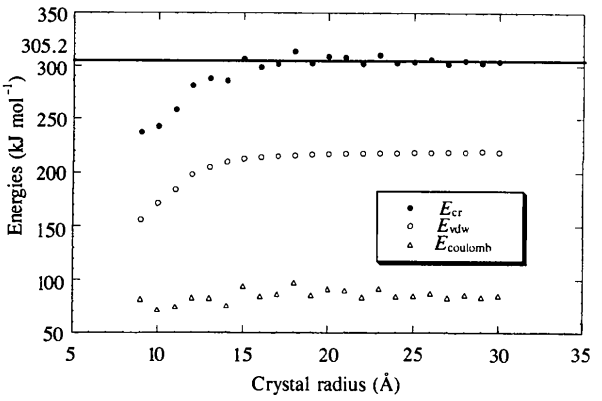


Fig. 6. Contributions of coulombic and van der Waals interaction energies to the lattice energy $E_{cr}$.

The authors are indebted to Biosym Technologies for providing a licence lending, Rhône-Poulenc Industrialization for financial support, C. Vergelati (Rhône-Poulenc CRIT-C) for stimulating discussions and M. A. Perrin (Rhône-Poulenc CRA) for running the *GAUSSIAN* calculations.

## References

Baughman, R. G., Sams, D. D., Helland, B. J. & Jacobson, R. A. (1980). *Cryst. Struct. Commun.* **9**, 885–889.

Berkovitch-Yellin, Z. (1985). *J. Am. Chem. Soc.* **107**, 8239–8253.

Biosym Technologies (1993). *Solid State User's Guide.* Version 1.0. Biosym Technologies, San Diego, USA.

Black, S. N., Davey, R. J. & McLean, T. D. (1988). *Mol. Cryst. Liq. Cryst. Inc. Nonlinear Opt.* **161**, 283–290.

Black, S. N., Williams, L. J., Davey, R. J., Moffatt, F., McEwan, D. M., Docherty, R. & Williams, D. J. (1990). *J. Phys. Chem.* **94**, 3223–3226.

Bondi, A. (1968). *Physical Properties of Molecular Crystals, Liquids, and Glasses.* New York: John Wiley & Sons, Inc.

Bravais, A. (1913). Etudes Cristallographiques, Paris.

Cadiergue, H. (1992). Thesis. University of Aix-Marseille III, France.

Dauber-Osguthorpe, P., Roberts, V. A., Osguthorpe, D. J., Wolff, J., Genest, M. & Hagler, A. T. (1988). *Proteins Struct. Funct. Genet.* **4**, 31–47.

Davey, R. J., Black, S. N., Logan, D., Maginn, S. J., Fairbrother, J. E. & Grant, D. J. W. (1992). *J. Chem. Soc. Faraday. Trans.* **88**(23), 3461–3466.

Docherty, R., Clydesdale, G., Roberts, K. J. & Bennema, P. (1991). *J. Phys.* **24**, 89–99.

Donnay, J. D. H. & Harker, D. (1937). *Am. Mineral.* **22**, 446.

Dowty, E. (1980). *Am. Mineral.* **65**, 465–471.

Friedel, G. (1907). *Bull. Soc. Fr. Minéral.* **30**, 326.

Hartman, P. (1980). *J. Cryst. Growth*, **49**, 157–165.
Hartman, P. & Bennema, P. (1980). *J. Cryst. Growth*, **49**, 145–156.
Hartman, P. & Perdok, W. G. (1955*a*). *Acta Cryst.* **8**, 49–52.
Hartman, P. & Perdok, W. G. (1955*b*). *Acta Cryst.* **8**, 521–524.
Lennard-Jones, J. E. (1924). *Proc. R. Soc. London Ser. A*, **106**, 442.
Pfefer, G., Boistelle, R. & Sabbah, R. (1996). In preparation.
Van der Voort, E. (1990). Thesis. University of Nijmegen, The Netherlands.
Wiberg, K. B. & Breneman, C. M. (1990). *J. Comput. Chem.* **11**, 361.
Woensdregt, C. F. (1992). *Z. Kristallogr.* **201**, 1–7.
Wulff, G. (1901). *Z. Kristallogr.* **34**, 449.